International Journal of Thermophysics, Vol. 24, No. 2, March 2003 (© 2003)

Isochoric Heat Capacity Measurements for 0.5 H_2O + 0.5 D_2O Mixture in the Critical Region

N. G. Polikhronidi,[1] I. M. Abdulagatov,[1–3] J. W. Magee,[2] and G. V. Stepanov[1]

Received September 4, 2002

The isochoric heat capacity C_V of an equimolar $H_2O + D_2O$ mixture was measured in the temperature range from 391 to 655 K, at near-critical liquid and vapor densities between 274.05 and 385.36 $kg \cdot m^{-3}$. A high-temperature, high-pressure, nearly constant-volume adiabatic calorimeter was used. The measurements were performed in the one- and two-phase regions including the coexistence curve. The uncertainty of the heat-capacity measurement is estimated to be $\pm 2\%$. The liquid and vapor one- and two-phase isochoric heat capacities, temperatures, and densities at saturation were extracted from the experimental data for each measured isochore. The critical temperature and the critical density for the equimolar $H_2O + D_2O$ mixture were obtained from isochoric heat capacity measurements using the method of quasi-static thermograms. The measurements were compared with a crossover equation of state for $H_2O + D_2O$ mixtures. The near-critical isochoric heat capacity behavior for the 0.5 H_2O + 0.5 D_2O mixture was studied using the principle of isomorphism of critical phenomena. The experimental isochoric heat capacity data for the 0.5 H_2O + 0.5 D_2O mixture exhibit a weak singularity, like that of both pure components. The reliability of the experimental method was confirmed with measurements on pure light water, for which the isochoric heat capacity was measured on the critical isochore (321.96 $kg \cdot m^{-3}$) in both the one- and two-phase regions. The result for the phase-transition temperature (the critical temperature, $T_{C,\ \text{this work}} = 647.104 \pm 0.003$ K) agreed, within experimental uncertainty, with the critical temperature ($T_{C,\ \text{IAPWS}} = 647.096$ K) adopted by IAPWS.

KEY WORDS: adiabatic calorimeter; coexistence curve; critical point; crossover equation of state; heavy water; isochoric heat capacity; light water; mixture.

[1] Institute of Physics of the Dagestan Scientific Center of the Russian Academy of Sciences, M. Yaragskogo Str. 94, 367005 Makhachkala, Dagestan, Russia.

[2] Physical and Chemical Properties Division, National Institute of Standards and Technology, 325 Broadway, Boulder, Colorado 80305, U.S.A.

[3] To whom correspondence should be addressed. E-mail: ilmutdin@boulder.nist.gov

0195-928X/03/0300-0405/0 © 2003 Plenum Publishing Corporation

1. INTRODUCTION

Thermodynamic property measurements on isotopic solutions are essential to improve our knowledge of mixture critical behavior [1]. Also, measurements can shed light on other theoretical problems connected with the critical behavior of solutions of isotopes, for example, the degree to which isotope exchange reactions will affect near-critical and supercritical thermodynamic property behavior [1].

Thermodynamic property measurements of H_2O+D_2O mixtures are scarce, but are particularly rare for the near-critical and the supercritical regions. Simonson [2] has reported the excess enthalpy H^E of H_2O+D_2O mixtures in a range of temperature from 310 to 673 K at pressures from 7 to 37 MPa. Marshall and Simonson [3] have reported liquid + vapor critical temperatures of H_2O+D_2O mixtures over the entire composition range with a precision of $\pm$ 0.1 K. The critical temperatures $T_C(x)$ of H_2O+D_2O mixtures were shown, within uncertainties, to follow a linear function of the concentration x, given by $T_C(x) = 647.14 - 3.25x$ [3], although Marshall and Simonson [3] argued that the excess enthalpy causes a slight deviation of the linear behavior of the critical temperature curve. But the slight deviation is of the same order of the experimental uncertainty. There are no reported experimental data for the critical pressure and the critical density. Bazaev et al. [4] have reported $PVTx$ measurements for H_2O+D_2O mixtures in the critical and supercritical regions for two compositions, 0.5 and 0.6 mole fraction of D_2O.

Crossover equations of state of the H_2O+D_2O mixture for the Helmholtz-energy density have been developed by Abdulkadirova et al. [1] and by Kiselev et al. [5]. Both crossover models incorporate a crossover from fluctuation-induced scaling behavior near the critical curve to regular (classical or mean-field, Landau expansion) behavior outside the critical region. The first of these models [1] is a generalization of a crossover equation of state previously developed by Kostrowicka Wyczalkowska et al. [6] for pure H_2O and pure D_2O, which was extended to mixtures by applying the principle of isomorphism of the critical behavior. Two parameters ($\bar{u}$ and Λ) govern the crossover from asymptotic singular critical behavior (nonclassical) to mean-field (classical) critical behavior of the Helmholtz energy density. This crossover model represents the thermodynamic properties of H_2O+D_2O mixtures in the same range of temperatures and densities as for the pure components, i.e., reduced susceptibility $\bar{\chi}^{-1} < 2$, density $\rho > 165\ \mathrm{kg \cdot m^{-3}}$, and temperature $T > 630$ K. The second of these crossover equations was developed for H_2O+D_2O mixtures by Kiselev et al. [5], who applied an isomorphic generalization of the law of corresponding states (LCS) to the prediction of thermodynamic properties

and phase behavior of H_2O+D_2O mixtures in a wide region around the locus of vapor+liquid critical points. This model yields a resonable representation of available thermodynamic property data over the following ranges of temperature $0.8T_C(x) < T < 1.5T_C(x)$ and density $0.35\rho_C(x) < \rho < 1.65\rho_C(x)$. Both crossover models represent thermodynamic property data with comparable accuracy.

A key difference between the two approaches is that, for the model of Abdulkadirova et al. [1], the coefficients in the scaling fields and the crossover parameters are identical for H_2O and D_2O and are independent of ζ (field variable related to mole fraction x), while for the crossover model of Kiselev et al. [5], the adjustable parameters in the equation for pure D_2O differ from those in the equation for pure H_2O. Both models under consideration, developed by Kiselev et al. [5] (LCS crossover model) and by Abdulkadirova et al. [1] (principle of the critical—point universality for binary fluids), were based on pure-component data, limited experimental data on the critical properties, and experimental excess enthalpies [2] for H_2O+D_2O mixtures. Such limited experimental information for mixtures of H_2O and D_2O may not be adequate to unambiguously determine the parameters for a crossover equation of state of these mixtures in the critical region. Experimental measurements for the specific heat capacity C_V of mixtures of H_2O and D_2O are, therefore, needed to check the reliability of the proposed equation of state for H_2O+D_2O mixture.

Due to an absence of adequate experimental ($PVTx$ and C_VVTx) data, it is not possible to understand the effect of isotopic exchange reaction on the thermodynamic behavior of the H_2O+D_2O system and to develop an accurate scaling equation of state. In this work, we will report measured C_VVTx properties for an equimolar 0.5 H_2O+0.5 D_2O mixture. We have used a high-temperature, high-pressure nearly constant-volume adiabatic calorimeter over ranges of temperature between 391 and 655 K and density from 274.05 to 385.36 $kg \cdot m^{-3}$. These new data together with our previous $PVTx$ measurements [4] will improve the experimental thermodynamic database and promote the development of a high accuracy crossover equation of state for the H_2O+D_2O mixture system. In previous work, we have reported isochoric heat-capacity data for the pure components, H_2O and D_2O, near the critical and supercritical regions [7, 8]. The same apparatus was used in the present work to measure C_V for the H_2O+D_2O mixture. To confirm the accuracy of this method, isochoric heat capacity measurements were made on a pure sample of light water very near the critical isochore 321.96 $kg \cdot m^{-3}$ ($\rho_{C,\,IAPWS} = 322.00\ kg \cdot m^{-3}$). The measured values of C_V for pure H_2O will be compared with a crossover model [9], with the IAPWS-95 [10] formulation, and with previously reported high-accuracy

experimental isochoric heat capacity data. The predictive capabilities of the crossover models reported by Abdulkadirova et al. [1] and Kiselev et al. [5] will be tested using the present experimental isochoric heat-capacity data for the $H_2O + D_2O$ mixture.

2. EXPERIMENTAL

The experimental apparatus used for the present isochoric heat-capacity measurements is the same as that used for the measurements on the pure components H_2O and D_2O [7, 8]. The apparatus and procedures that were described previously [7, 8, 11] were used without modification. Since the apparatus, the construction of the calorimeter, the experimental procedure, and the uncertainty estimates have been described in detail in several previous publications [7, 8, 11], they will be only briefly reviewed here.

The isochoric heat capacities were measured with a high-temperature, high-pressure, adiabatic, and nearly constant-volume calorimeter, which gives an uncertainty of 2 to 3% of the heat capacity. The volume of the calorimeter, 105.126 ± 0.05 cm^3 (at atmospheric pressure and 297.15 K), was determined by using PVT data for pure water [10] as a function of temperature and pressure. In this experiment, the uncertainty in the determination of volume at a given T and P is approximately 0.05%. The mass of the sample was measured by using a weighing method with an uncertainty of 0.05 mg. The sample was prepared gravimetrically to give a composition of 0.500 mole fraction H_2O, with an uncertainty of 0.001 mole fraction Thus, the overall uncertainty in the measurements of density $\rho = m/V(P, T)$ is about 0.06%.

The heat capacity was obtained from measurements of the following: m, mass of the fluid; ΔQ, electrical energy released by the inner heater; ΔT, temperature change resulting from addition of an energy ΔQ; and C_0, heat capacity of the empty calorimeter. The heat capacity of the empty calorimeter C_0 was determined experimentally using a reference substance (helium-4) with well-known isobaric heat capacities [12], in the temperature range up to 1000 K at pressures up to 20 MPa. The uncertainty in the C_P data used for calibration of C_0 is 0.2%. A correction related to the cell's stretching behavior during a heating interval was determined with an uncertainty of about 4.0 to 9.5%, depending on the density. The absolute uncertainty in C_V due to small deviations from perfect adiabatic control is 0.013 kJ·K^{-1}. The combined standard uncertainty related to the indirect character of the C_V measurements did not exceed 0.16%. The thermometer was calibrated on the ITS-90 scale. The uncertainty of the temperature measurements is less than 10 mK. Based on a detailed analysis of all

sources of uncertainty likely to affect the determination of C_V with the present method, the combined standard uncertainty of measuring the heat capacity with allowance for the propagation of uncertainty related to the stretching of the cell is $\pm 2\%$.

The heat capacity was measured as a function of temperature at nearly constant density. The calorimeter was filled at room temperature, sealed off, and heated along a quasi-isochore. Each run normally started in the two-phase region and was completed in the one-phase region. This method enables one to determine, with good accuracy, the transition temperature T_S of the system from the two-phase to a single-phase state (i.e., to determine T_S and ρ_S data corresponding to the phase-coexistence curve), the jump in the heat capacity ΔC_V, and reliable C_V data in the single- and two-phase regions (see Polikhronidi et al. [11]). The temperature T_S and density ρ_S at coexistence was determined by the method of quasi-static thermograms as described in detail in previous publications [11, 13]. The method of quasi-static thermograms makes it possible to obtain reliable data to within ± 0.01 K from the critical temperature T_C with an uncertainty of 0.01 to 0.02 K. The water was triple-distilled and degassed, and had an electric conductivity of about 10^{-4} $\Omega^{-1} \cdot m^{-1}$. The purity of D_2O was 99.9 mol%.

3. RESULTS AND DISCUSSION

Measurements of the isochoric heat capacity for the equimolar H_2O+D_2O mixture were performed along two liquid and five vapor isochores, namely, 274.05, 299.58, 318.07, 334.78, 338.98 (the critical density), 352.11, and 385.36 $kg \cdot m^{-3}$. The temperature range was 391 to 655 K. In total, 471 C_V measurements were made in the one- and two-phase regions. On the coexistence curve, a total of 21 values of C_V and (T_S, ρ_S) was measured. The experimental one- and two-phase C_V data and (C_{V1}, C_{V2}, T_S, ρ_S) values on the coexistence curve are presented in Tables I and II and shown in Figs. 1a–1d, 2a, and 2b. The critical temperature $T_C = 645.47$ K for this mixture ($x = 0.5$ mole fraction of D_2O) was found by Marshall and Simonson [3]. As there are no experimental data for the critical pressure and the critical density, in the crossover equations of state for the equimolar mixture 0.5 H_2O+0.5 D_2O, Abdulkadirova et al. [1] and Kiselev et al. [5] assumed that these parameters are linear as a function of the mole fraction x. Therefore, according to this assumption, the critical density and the critical pressure for 0.5 H_2O+0.5 D_2O mixture are $\rho_C = 338.99$ $kg \cdot m^{-3}$ and $P_C = 21.8675$ MPa. Figures 1a–1d shows the temperature dependence of the measured isochoric heat capacities for the

Table I. Experimental One-Phase and Two-Phase Isochoric Heat Capacities for a 0.500 (±0.001) mole fraction $H_2O + 0.500$ mole fraction D_2O Mixture at Near-Critical Densities

T (K)	C_V (kJ·kg^{-1}·K^{-1})	T (K)	C_V (kJ·kg^{-1}·K^{-1})	T (K)	C_V (kJ·kg^{-1}·K^{-1})
$\rho = 385.36$ kg·m^{-3}		644.98	13.183	642.13	9.799
		645.06	13.719	642.22	9.709
391.12	4.077	645.14	14.327	642.31	9.789
391.44	4.074	645.16	14.481	642.40	9.872
477.32	4.563	645.18	14.644	642.49	9.869
477.61	4.566	645.23	15.086	642.76	10.031
524.68	5.042	645.26	15.423	642.85	10.226
525.05	5.046	645.28	15.078	642.94	10.181
525.33	5.040	**645.295**[a]	**15.891**[a]	643.02	10.210
575.32	5.980	**645.295**[a]	**8.179**[a]	643.11	10.263
575.68	5.982	645.31	7.879	644.63	11.833
576.21	6.001	645.40	7.537	644.72	12.109
580.81	6.112	645.48	7.012	644.81	12.590
581.07	6.155	645.56	6.493	644.90	12.755
613.41	7.081	645.73	5.908	644.99	13.170
613.67	7.094	645.99	5.270	645.08	13.740
613.93	7.103	646.07	5.219	645.17	14.746
631.79	8.244	646.15	5.022	645.26	15.338
632.38	8.271	646.24	4.965	645.35	16.657
634.44	8.423	646.32	4.911	**645.424**[a]	**20.455**[a]
634.59	8.517	646.40	4.853	**645.424**[a]	**9.239**[a]
634.86	8.428	646.49	4.798	645.53	8.061
640.09	9.381	646.57	4.746	645.62	7.192
640.34	9.320	646.74	4.740	645.71	7.094
640.51	9.403	646.82	4.734	645.80	6.408
641.10	9.655	646.91	4.744	645.88	6.378
641.35	9.727	646.99	4.756	645.97	6.208
641.52	9.735	647.08	4.750	646.06	6.213
641.94	9.717	647.16	4.752	646.15	6.086
642.03	9.712	647.24	4.748	646.24	5.970
642.11	9.670	647.33	4.760	646.33	5.878
642.20	9.779			646.42	5.861
642.37	9.750	$\rho = 352.11$ kg·m^{-3}		646.51	5.840
642.45	9.848	634.07	8.250		
642.62	10.00	634.16	8.276	$\rho = 338.98$ kg·m^{-3}	
642.70	9.978	634.25	8.410	500.80	6.347
642.79	10.234	634.34	8.398	585.48	6.332
642.87	10.276	634.43	8.452	585.74	6.347
643.96	10.880	634.52	8.381	586.09	6.351
644.28	11.214	634.61	8.448	583.56	6.342
644.64	11.928	634.70	8.475	584.85	6.338
644.72	12.083	638.28	8.983	584.42	6.346
644.81	12.259	638.46	9.168	608.93	7.008

Table I. *(Continued)*

T (K)	C_V (kJ·kg^{-1}·K^{-1})	T (K)	C_V (kJ·kg^{-1}·K^{-1})	T (K)	C_V (kJ·kg^{-1}·K^{-1})
609.45	7.017	645.65	8.204	643.38	11.217
620.45	7.442	645.73	7.843	643.47	11.138
620.71	7.456	645.90	7.217	643.54	11.172
620.88	7.449	616.15	6.819	643.65	11.267
621.05	7.460	616.24	6.733	643.74	11.367
632.64	8.363	616.32	6.642	643.83	11.436
632.89	8.399	646.91	6.208	643.92	11.524
633.06	8.420	646.99	6.153	644.01	11.682
633.24	8.434	647.11	6.080	644.10	11.751
636.88	8.917	648.76	5.608	644.19	11.724
637.05	8.929	648.84	5.611	644.28	12.064
637.13	8.913	648.92	5.603	644.37	12.127
637.30	8.952	649.09	5.601	644.46	12.556
637.38	9.008	649.17	5.598	644.54	12.715
641.02	9.573	649.26	5.580	644.63	13.201
641.19	9.730	652.27	5.342	644.72	13.448
641.27	9.786	652.36	5.319	644.81	13.528
641.44	9.893	652.44	5.354	644.90	14.065
641.52	9.922	652.61	5.329	644.99	14.268
642.36	10.183	652.78	5.298	645.08	14.738
642.53	10.248	$\rho = 334.78$ kg·m^{-3}		645.17	15.380
642.62	10.300			645.26	16.252
642.79	10.412	622.10	7.890	645.35	18.479
642.87	10.527	622.28	7.960	**645.449**[a]	**22.620**[a]
643.71	11.120	622.46	7.980	**645.449**[a]	**10.812**[a]
644.05	11.347	622.64	7.961	645.53	8.683
644.22	11.633	622.82	8.021	645.62	8.057
644.39	11.933	623.00	8.097	645.70	7.681
644.64	121.528	623.18	8.043	645.80	7.272
644.89	13.518	623.54	8.001	645.88	7.125
644.98	14.207	623.72	7.994	645.97	7.102
645.06	14.548	623.90	8.020	646.15	6.581
645.14	14.953	624.08	8.085	646.24	6.618
645.23	15.626	636.49	9.314	646.33	6.632
645.31	17.071	636.67	9.307	646.69	5.788
645.40	18.766	636.86	9.316	646.78	5.797
645.41	19.238	637.04	9.336	646.87	5.761
645.43	19.843	637.22	9.384	652.12	4.689
645.45	20.309	637.40	9.408	652.22	4.630
645.455[a]	**22.870**[a]	637.58	9.402	652.30	4.538
645.455[a]	**10.895**[a]	637.94	9.430	$\rho = 318.07$ kg·m^{-3}	
645.48	10.284	638.12	9.498		
645.50	10.073	638.29	9.506	535.10	5.310
645.55	9.017	638.47	9.590	535.28	5.318

Table I. *(Continued)*

T (K)	C_V (kJ·kg^{-1}·K^{-1})	T (K)	C_V (kJ·kg^{-1}·K^{-1})	T (K)	C_V (kJ·kg^{-1}·K^{-1})
535.56	5.313	645.65	7.005	637.97	9.596
585.57	6.235	645.73	6.702	641.94	10.384
585.92	6.247	645.82	6.400	642.20	10.359
603.91	6.883	645.91	6.107	642.45	10.681
603.26	6.960	645.98	6.002	642.53	10.703
624.30	8.247	646.07	5.903	642.70	10.822
624.56	8.243	646.15	5.819	642.87	10.907
625.58	8.334	646.24	5.724	643.04	11.004
626.09	8.362	646.32	5.661	643.92	11.803
632.39	8.748	646.41	5.599	644.22	12.233
637.22	9.423	646.49	5.556	644.30	12.483
637.38	9.437	646.57	5.514	644.47	12.603
637.55	9.462	646.66	5.460	644.55	13.037
637.72	9.460	646.74	5.417	644.64	13.284
639.92	9.733	646.83	5.381	644.81	13.753
640.17	9.806	646.91	5.355	644.89	14.217
640.34	9.818	646.99	5.320	644.98	14.581
640.51	9.831	647.08	5.286	645.06	15.025
642.11	10.321	650.60	4.880	645.14	15.594
642.37	10.487	650.68	4.885	645.23	16.358
642.53	10.502	650.77	4.865	645.24	16.501
642.62	10.556	650.85	4.877	645.26	16.750
643.63	11.373	650.93	4.888	**645.275**[a]	**17.155**[a]
643.71	11.439	651.02	4.891	**645.275**[a]	**8.727**[a]
643.88	11.561	651.10	4.895	645.31	8.207
644.05	11.835	651.18	4.898	645.35	7.649
644.30	12.298	651.27	4.900	645.40	7.479
644.47	12.724	651.35	4.904	645.48	7.033
644.55	12.993	651.44	4.912	645.56	6.495
644.72	13.680	651.52	4.910	645.65	6.158
644.89	14.227	651.60	4.924	645.73	5.956
644.98	14.412	651.69	4.940	645.90	5.528
645.14	15.268	651.77	4.931	646.07	5.221
645.25	16.355	651.86	4.936	646.24	5.023
645.30	17.160	651.94	4.958	646.40	4.944
645.35	18.000			646.57	4.820
645.40	19.326	$\rho = 299.58$ kg·m^{-3}		646.74	4.745
645.41	19.993			648.34	4.390
645.417[a]	**20.490**[a]	636.88	9.388	648.59	4.382
645.417[a]	**9.558**[a]	637.13	9.413	648.75	4.394
645.43	9.202	637.38	9.415	648.92	4.400
645.45	8.887	637.46	9.498	649.09	4.413
645.50	8.134	637.55	9.513	649.34	4.398
645.56	7.316	637.80	9.490	649.57	4.440

Table I. *(Continued)*

T (K)	C_V (kJ·kg^{-1}·K^{-1})	T (K)	C_V (kJ·kg^{-1}·K^{-1})	T (K)	C_V (kJ·kg^{-1}·K^{-1})
$\rho = 274.05$ kg·m^{-3}		644.30	13.345	645.40	5.204
		644.39	13.803	645.43	5.047
619.85	8.523	644.47	14.781	645.48	4.981
620.11	8.531	644.55	16.089	645.53	4.913
620.37	8.549	644.57	16.320	645.56	4.858
620.62	8.567	644.59	16.547	647.58	3.788
620.78	8.573	644.60	16.629	647.66	3.789
621.05	8.588	644.62	16.654	647.75	3.782
621.31	8.601	644.64	16.641	647.83	3.843
621.65	8.620	644.66	16.567	647.92	3.840
621.82	8.633	644.67	16.370	648.00	3.840
621.99	8.642	644.69	16.154	648.08	3.840
622.50	8.675	644.70	15.878	651.27	3.812
622.68	8.681	644.72	15.620	651.35	3.813
639.16	9.924	644.74	15.363	651.44	3.812
639.41	10.083	644.76	15.154	651.52	3.815
639.75	10.132	**644.773**[a]	**14.841**[a]	651.60	3.819
639.92	10.207	**644.773**[a]	**8.805**[a]	651.69	3.820
640.00	10.239	644.79	7.922	651.47	3.820
640.17	10.264	644.81	8.083	651.86	3.820
640.34	10.332	644.82	7.644	651.94	3.820
640.51	10.378	644.84	7.228	654.03	3.823
642.37	10.951	644.86	7.168	654.11	3.827
642.62	11.065	644.87	7.106	654.20	3.830
642.87	11.193	644.89	7.025	654.28	3.831
643.21	11.404	644.97	6.513	654.36	3.830
643.63	11.802	645.06	6.105	654.45	3.832
643.71	11.884	645.14	5.768	654.53	3.835
643.80	11.982	645.23	5.560	654.61	3.833
644.05	12.478	645.31	5.399	654.70	3.830
644.14	12.713			654.78	3.830

[a] Saturation point.

equimolar mixture of H_2O+D_2O along the near-critical densities together with the values calculated with the LCS crossover model of Kiselev et al. [5]. The experimental values of liquid and vapor one-phase (C'_{V1}, C''_{V1}) and liquid and vapor two-phase (C'_{V2}, C''_{V2}) isochoric heat capacities on the coexistence curve are shown in Figs. 2a and 2b. Tightly spaced measurements were carried out in the critical region and near all phase transitions. This is essential for accurate determinations of the critical parameters and the phase transition curve that will promote the development of a better crossover equation of state.

Table II. Experimental Isochoric Heat Capacities (C'_{V1}, C''_{V1}), Temperatures (T_S), and Densities (ρ_S) of H_2O and an Equimolar Mixture of $H_2O + D_2O$ on the Saturation Boundary

T_S (K)	ρ_C (kg·m^{-3})	C_{V1} (kJ·kg^{-1}·K^{-1})	C_{V2} (kJ·kg^{-1}·K^{-1})
		H_2O	
647.104	321.96	10.876	23.917
647.109	321.96	10.843	24.628
		0.50 mole fraction H_2O + 0.50 mole fraction D_2O	
	ρ_S (kg·m^{-3})		
644.773	274.05	8.805	14.841
645.275	299.58	8.727	17.155
645.417	318.07	9.558	20.490
645.449	334.78	10.812	22.620
645.455	338.98	10.895	22.875
645.424	352.11	9.239	20.703
645.295	385.36	8.178	15.891

Mixture measurements often present new challenges, not present for pure components, including some empirical artifacts that can be difficult to explain. Figure 1d shows the temperature dependence of two-phase C_V near the dew-point temperature for a vapor isochore (274.05 kg·m^{-3}). In a temperature interval of 0.75 K just below the dew point, between 644.5 K and the saturation temperature $T_S = 644.773$ K, we observed anomalous behavior. A rounded but pronounced C_V maximum was observed at a temperature of 644.55 K, which had not been seen for either pure component (Amirkhanov et al. [14], Kerimov [15], Abdulagatov et al. [16], Polikhronidi et al. [7, 8], and Mursalov et al. [17]). A reasonable speculation is that the rounded maximum is due to a pre-transition phenomenon, such as de-mixing that forms a new phase of different composition. When temperatures are just above the dew point temperature, a different pre-transition phenomenon has been observed that is called pre-condensation. In the present case, we will refer to pre-evaporation. Pre-evaporation behavior was previously reported for aqueous salt solutions by Abdulagatov et al. [18] and has also been recently seen in CO_2 + *n*-decane and H_2O + *n*-hexane mixtures by Polikhronidi et al. [19] and Kamilov et al. [20]. It was noted that this anomaly vanished as the density was increased toward the critical density. A probable explanation is that as the critical density is approached, the effect of critical fluctuations on the temperature dependence of C_V predominates over the pre-evaporation phenomenon that

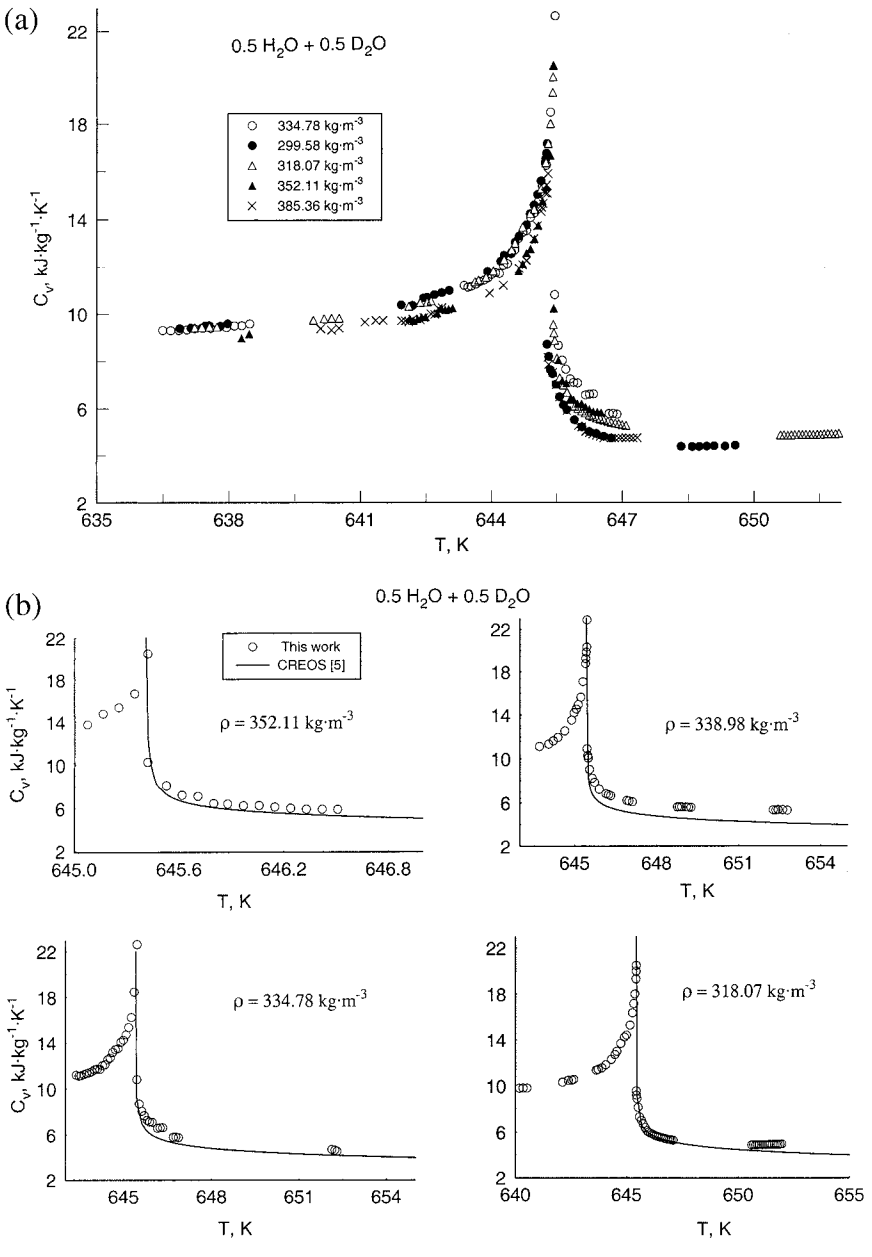

Fig. 1. (a)–(b) one-phase and two-phase isochoric heat capacities of an equimolar H_2O+D_2O mixture as a function of temperature along the near-critical isochore; the solid lines represent the values of C_V calculated from the LCS crossover model of Kiselev et al. [5].

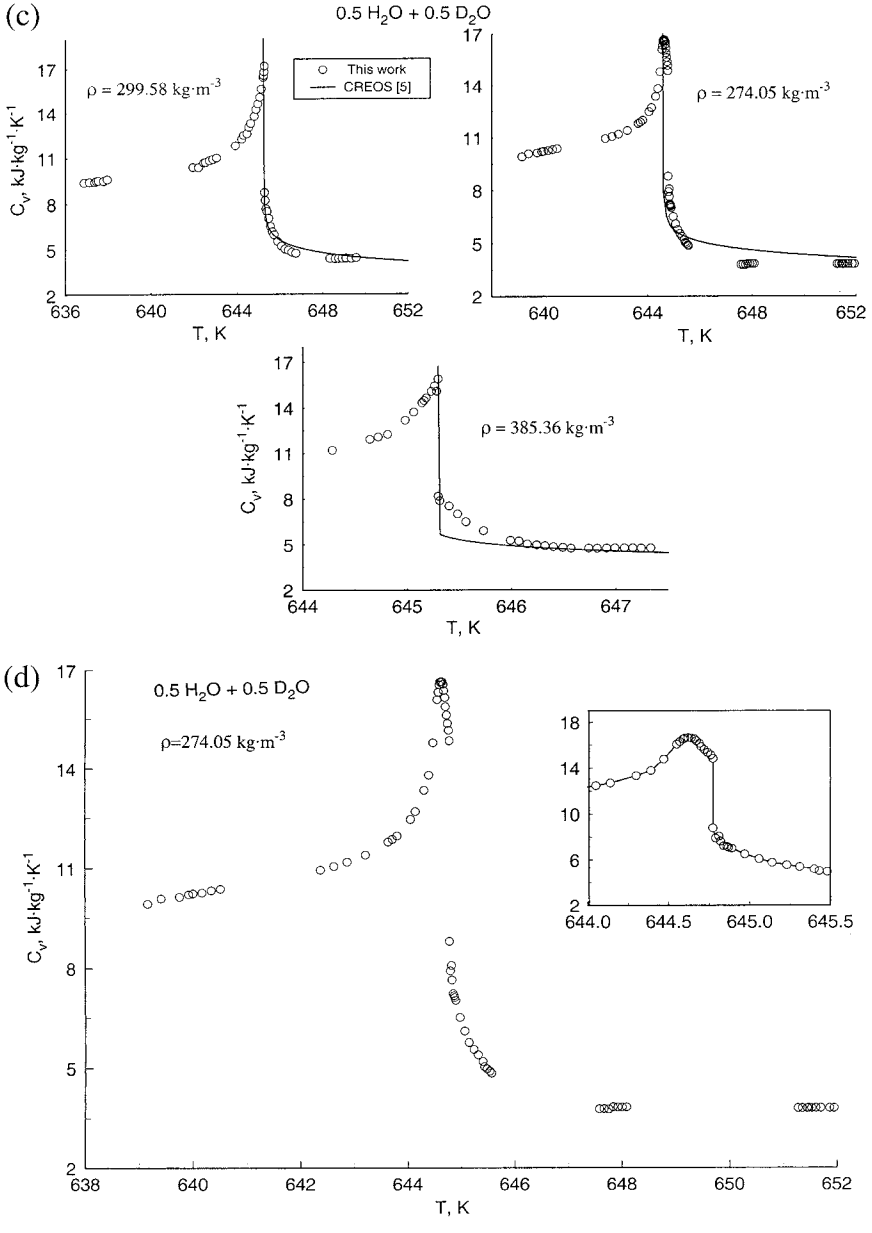

Fig. 1. *(Continued).*

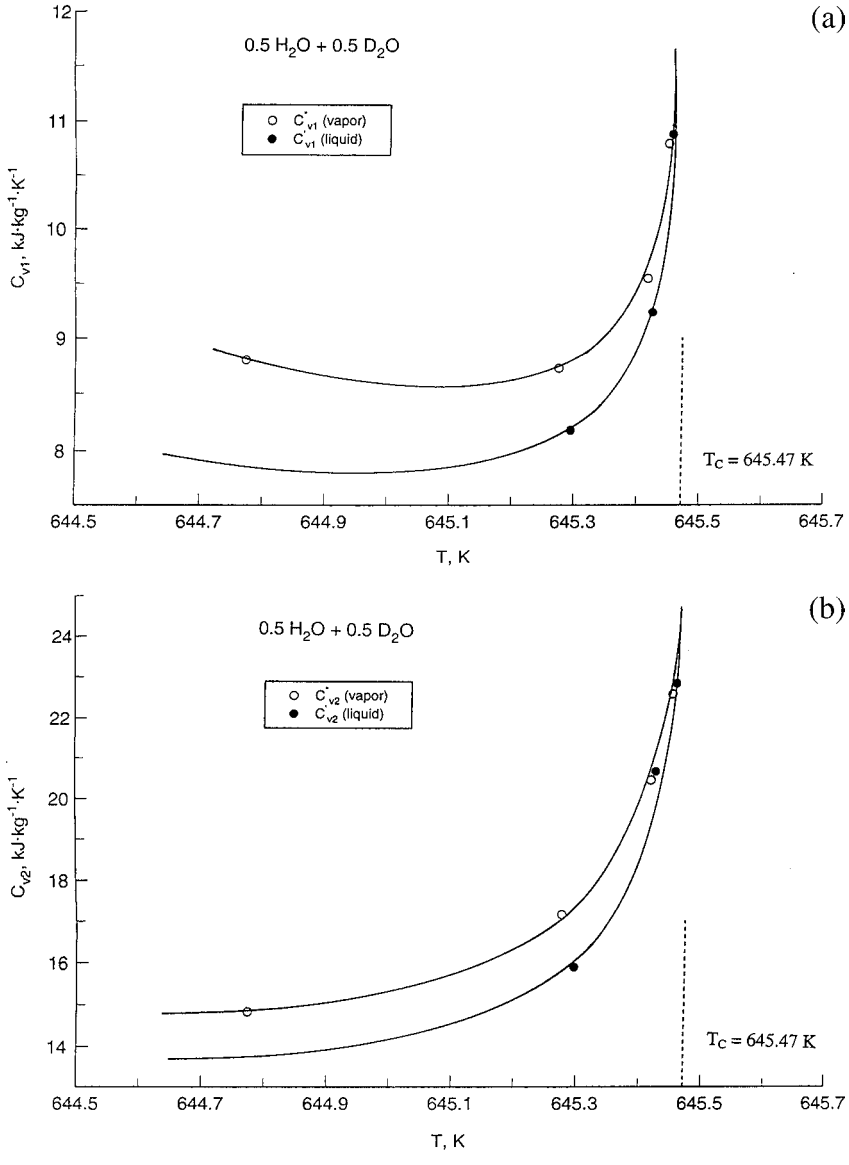

Fig. 2. Experimental values of (a) liquid and vapor one-phase (C'_{V1}, C''_{V1}) and (b) two-phase (C'_{V2}, C''_{V2}) isochoric heat capacities for an equimolar H_2O+D_2O mixture on the coexistence curve as a function of temperature near the critical point; solid curves are provided as a guide for the eye.

caused the rounded maximum two-phase C_V anomaly near the phase-transition curve.

The density dependence of C_V for the equimolar H_2O+D_2O mixture along three supercritical isotherms is depicted in Fig. 3 together with values calculated from the LCS crossover model of Kiselev et al. [5]. Figure 4 shows the temperature dependence of the measured values of isochoric heat capacity of the 0.5 H_2O+0.5 D_2O mixture and their pure components (pure light and heavy water) calculated from the parametric crossover model of Kiselev and Friend [9] at the critical density. At low temperatures ($T < 640$ K) in the two-phase region, the values of C_V for pure light and heavy water and their mixture show only very small differences, while in the one-phase region at temperatures above 648 K the experimental C_{VX} for the mixture is slightly higher than values of C_V for either pure light or heavy water. A similar temperature dependence was found for C_{VX} of the 0.5 H_2O+0.5 D_2O mixture and for C_V of both pure components.

Figures 5a and b depict the measured vapor-liquid coexistence curve ($T_S-\rho_S$) for the 0.5 H_2O+0.5 D_2O mixture that was determined from the C_V measurements by applying the method of quasi-static thermograms [11, 13] and for pure components near the critical point together with values calculated from the LCS crossover model by Kiselev et al. [5]. The

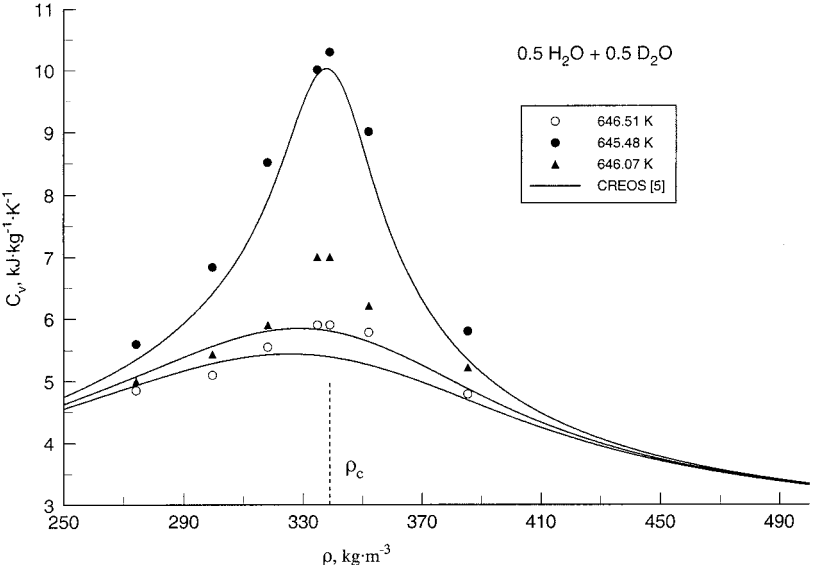

Fig. 3. Experimental isochoric heat capacity of an equimolar H_2O+D_2O mixture as a function of density along supercritical isotherms together with values calculated from the LCS crossover model by Kiselev et al. [5].

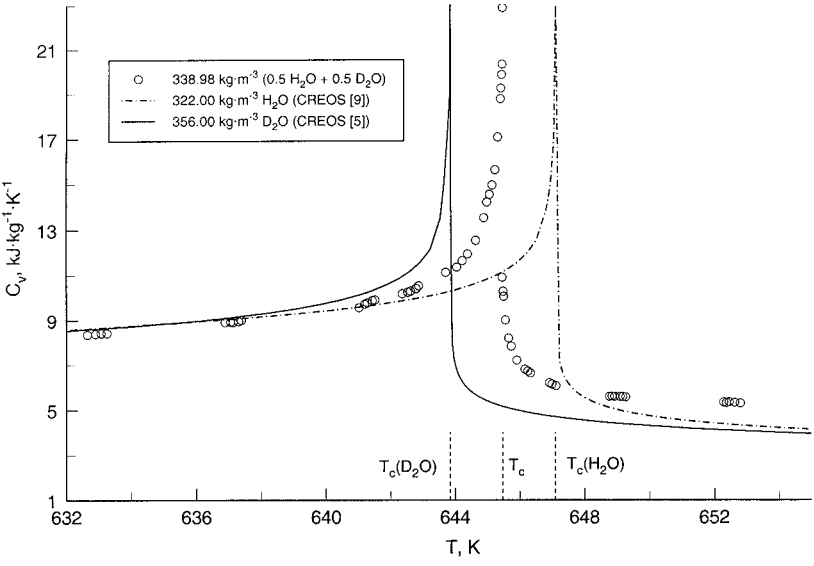

Fig. 4. Experimental and calculated values of isochoric heat capacities of the 0.5 H_2O+ 0.5 D_2O mixture and their pure components (H_2O and D_2O) along each critical isochore as a function of temperature.

agreement is good (deviations for saturated density values are within 2.5%, and deviations for saturated temperature values are within 0.025 K) except for two vapor isochores (274.05 and 299.58 $kg \cdot m^{-3}$). The deviations in saturated temperature values for these vapor isochores are 0.277 and 0.095 K, respectively (deviations for saturated densities are $< 3\%$). This agreement is still good because the crossover equation [5] was developed without using any experimental data for H_2O+D_2O mixtures. Figure 5b shows comparisons in the $T_S - \rho_S$ plane for the 0.5 H_2O+0.5 D_2O mixture with values calculated from a new crossover equation of state with parameters of the regular parts fitted with the present C_{VX} data. As one can see from this figure, the agreement of experimental data with the fitted crossover model is much better (deviations for densities are about 1.5%) than for the LCS crossover model [5]. Our new measurement of the saturation temperature $T_S = 645.455$ K (ITS-90) on an isochore (338.98 $kg \cdot m^{-3}$) very near the critical density is in close agreement (deviation of only 0.027 K and close to its experimental uncertainty of 0.02 K) with the values of the critical temperature $T_C = 645.428$ K (ITS-90) reported by Marshall and Simonson [3] for the same composition. This helps to confirm the reliability of the coexistence curve ($T_S - \rho_S$) near the critical point for the 0.5 H_2O+ 0.5 D_2O mixture, shown in Figs. 5a and b. Therefore, from our experimental

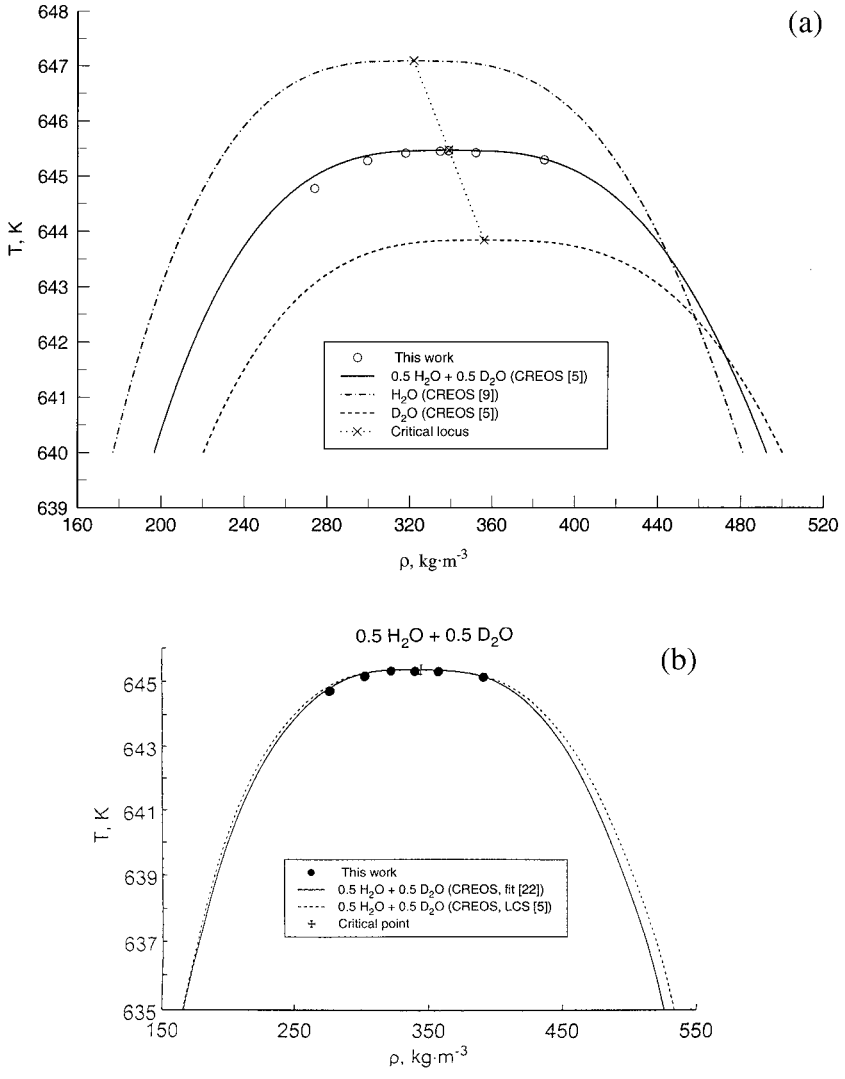

Fig. 5. Experimental and calculated liquid and vapor densities at saturation (a) for an equimolar H_2O+D_2O mixture and their pure components from C_V experiments together with values calculated from the LCS crossover models by Kiselev et al. [5, 9] in the temperature range (a) far from the critical point and (b) in the critical region.

$T_S - \rho_S$ data for the equimolar $H_2O + D_2O$ mixture at saturation, we have deduced values of the critical temperature T_C and the critical density ρ_C. Our results are: $T_C = 645.455 \pm 0.02$ K and $\rho_C = 338.98 \pm 0.05$ kg·m^{-3}.

Figure 6 shows selected data for experimental isochoric heat capacities from the literature on the critical isochore for pure H_2O together with values measured in this work, presented in Table III, on the 321.96 kg·m^{-3} isochore. The measured values (and their reproducibilities) of phase transition temperatures $T_{S,\text{this work}} = 647.104 \pm 0.003$ K (run-1) and $T_{S,\text{this work}} = 647.109 \pm 0.003$ K (run-2) for this isochore are in good agreement with a value of the critical temperature $T_{C,\text{IAPWS}} = 647.096$ K adopted by IAPWS [10] for the thermodynamic properties of light water. Figure 6 also shows the values of C_V calculated from the crossover equation by Kiselev and Friend [9] and from the IAPWS-95 formulation [10]. As shown by Fig. 6, the consistency between the present and previous measurements is good, except for a few data points reported by Kerimov [15] in the immediate vicinity of the phase transition temperature in the one-phase region. The IAPWS-95 formulation [10] shows good agreement (within 6%) in the critical region and systematic positive deviations (within 10%) in the range of regular C_V behavior. The LCS crossover model by Kiselev et al. [5]

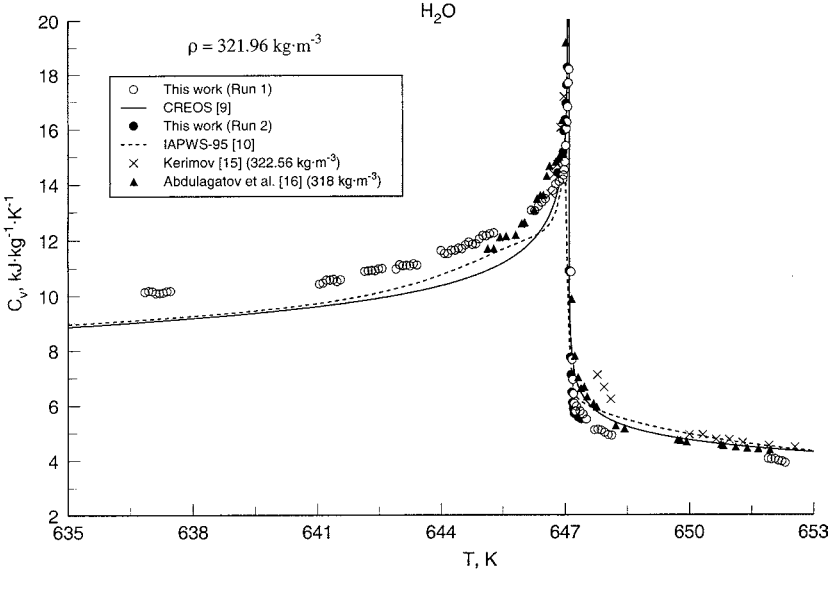

Fig. 6. Experimental and calculated values of isochoric heat capacities for pure light water on the critical isochore together with values calculated from the crossover equation of state (CREOS) [9] and IAPWS [10] formulations.

Table III. Experimental One-Phase and Two-Phase Isochoric Heat Capacities of Pure Light Water on the Critical Isochore

$\rho_C = 321.96\ \mathrm{kg \cdot m^{-3}}$			
T (K)	C_V ($\mathrm{kJ \cdot kg^{-1} \cdot K^{-1}}$)	T (K)	C_V ($\mathrm{kJ \cdot kg^{-1} \cdot K^{-1}}$)
Run-1		644.890	12.028
		644.974	12.153
636.805	10.140	645.058	12.139
636.893	10.178	645.142	12.208
636.980	10.163	645.238	12.245
637.067	10.090	646.152	13.048
637.154	10.096	646.236	13.031
637.241	10.117	646.320	13.186
637.328	10.168	646.404	13.337
637.415	10.172	646.488	13.461
641.017	10.428	646.666	13.756
641.101	10.461	646.740	13.995
641.186	10.574	646.824	14.088
641.270	10.568	646.908	14.163
641.354	10.592	646.924	14.317
641.439	10.517	646.942	14.509
641.523	10.584	646.958	14.800
642.113	10.885	646.975	15.382
642.198	10.898	646.992	15.984
642.282	10.911	647.009	16.228
642.366	10.900	647.026	16.781
642.450	10.971	647.042	17.657
642.534	10.979	647.059	18.155
642.871	10.954	647.076	20.142
642.956	11.113	647.093	22.347
643.040	11.077	**647.109**[a]	**24.628**[a]
643.124	11.091	**647.109**[a]	**10.843**[a]
643.208	11.068	647.126	7.655
643.292	11.142	647.143	6.934
643.377	11.099	647.160	6.409
643.964	11.614	647.177	6.070
644.049	11.512	647.195	5.794
644.133	11.509	647.212	5.774
644.217	11.626	647.230	5.960
644.301	11.624	647.314	5.790
644.385	11.703	647.389	5.682
644.469	11.681	647.473	5.493
644.553	11.816	647.667	5.102
644.638	11.912	647.748	5.127
644.722	11.832	647.831	5.091
644.806	11.852	647.915	5.008

Table III. *(Continued)*

$\rho_C = 321.96\ kg \cdot m^{-3}$			
T (K)	C_V ($kJ \cdot kg^{-1} \cdot K^{-1}$)	T (K)	C_V ($kJ \cdot kg^{-1} \cdot K^{-1}$)
648.000	4.925	647.007	16.322
648.083	4.901	647.025	16.919
651.855	4.058	647.042	17.584
651.939	4.033	647.059	18.241
652.025	4.047	647.075	20.317
652.106	3.984	647.092	21.642
652.193	3.955	**647.104**[a]	**23.917**[a]
652.274	3.901	**647.104**[a]	**10.876**[a]
	Run-2	647.125	7.742
		647.140	7.122
646.827	14.400	647.158	6.479
646.905	14.402	647.177	6.093
646.924	14.902	647.193	5.884
646.943	15.000	647.213	5.707
646.955	15.149	647.230	5.690
646.972	15.914	647.314	5.563
646.990	15.987	647.392	5.499

[a] Saturation point.

shows deviations up to 10% in the two-phase region far from the critical point ($T < 641$ K) while the agreement in the one-phase region is good (within 6%).

The experimental C_V data for the 0.5 H_2O+0.5 D_2O mixture were compared with the values calculated from crossover models developed by both Abdulkadirova et al. [1] (six-term Landau-expansion crossover model) and Kiselev et al. [5] (parametric LCS crossover model). Figures 1a to 1d show the experimental behavior of C_V as a function of temperature for the 0.5 H_2O+0.5 D_2O mixture at the various near-critical densities together with values calculated with the parametric LCS crossover model by Kiselev et al. [5] in the one-phase region. Note that the present data were not used to develop this model. Excellent agreement within 2.5% was found for the near-critical isochore of 318.07 $kg \cdot m^{-3}$ in the immediate vicinity of the phase-transition temperature while in the region far from the phase-transition temperature, the deviation was as large as 10%. Good agreement within 5.8% was found for the isochore of 299.58 $kg \cdot m^{-3}$. Excellent agreement, AAD=2.5%, was observed for the isochore of 385.36 $kg \cdot m^{-3}$ in the regular behavior region, and near saturation, the

deviations between measured and calculated values of C_V were as large as 10%. For the isochores of 352.11 and 334.78 $kg \cdot m^{-3}$, systematic positive deviations of 8 to 11%, respectively, were observed with a maximum deviation of 16%. Systematic positive deviations up to 16 to 20% were found for the 338.98 $kg \cdot m^{-3}$ isochore.

In order to improve the representation of the LCS crossover model by Kiselev et al. [5], only a re-fitting of the regular part parameters using the present experimental data would be advised. Figure 7 shows a comparison between the present experimental data along a near-critical isochore (334.78 $kg \cdot m^{-3}$) and values calculated from two versions of the parametric crossover model developed by Kiselev et al. [5]. The first version of the LCS crossover model was developed without experimental C_V data, and the second version uses the same equations with new parameters for the regular background part that were fitted with only the present C_V data without using any $PVTx$ data [21]. As shown in Fig. 7, the second version is in very good agreement (differences of 2 to 3%) with this work. A comparison between the present data and the values calculated from the six-term Landau expansion crossover model developed by Abdulakadirova et al. [1] is depicted in Fig. 8 for two selected near-critical densities (334.78 and 352.11 $kg \cdot m^{-3}$). Figure 8 also shows values calculated with the LCS

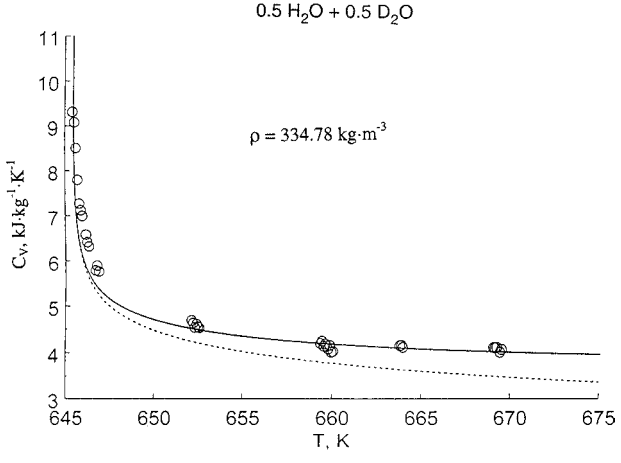

Fig. 7. Comparison of experimental isochoric heat capacity values of a 0.5 H_2O+0.5 D_2O mixture on the near-critical isochore (334.78 $kg \cdot m^{-3}$) with values calculated from the CREOS [5] (LCS crossover model, dashed curve) and the CREOS [21] with regular part parameters fitted to the present data (solid curve).

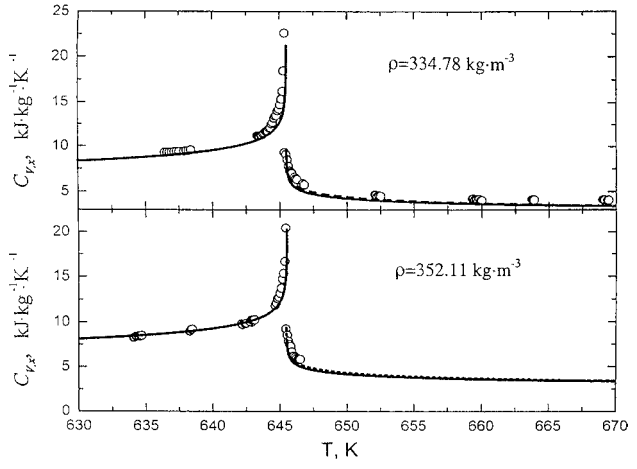

Fig. 8. Isochoric heat capacity of 0.5 H_2O+0.5 D_2O mixture along the two near-critical isochores 334.78 and 352.11 kg·m^{-3} together with values calculated from the CREOS [5] (LCS crossover model, dotted curve) and crossover equation of state by Abdulkadirova et al. [1] (solid curve).

version of the parametric crossover model by Kiselev et al. [5]. As one can see in Fig. 8, both crossover equations represent equally well the present isochoric heat capacity measurements for the 0.5 H_2O+0.5 D_2O mixture. This agrees with the finding of Abdulkadirova et al. [1] that both crossover models predict the thermodynamic properties of H_2O+D_2O mixtures with comparable accuracy.

The near-critical behavior of C_V for binary mixtures is controlled by the characteristic parameter K_2 [1]. This parameter is responsible for the deformation of the weak divergence of C_V and defines the range of Fisher renormalization of the critical exponents [22]. The isochoric heat capacity behavior of a binary mixture will exhibit the same behavior as those of a pure component in the range of temperature $\tau \gg \tau_2$ [1], where

$$\tau_2 = \left[A_0^+ \frac{K_2^2}{(x(1-x)} \right]^{1/\alpha}, \quad \Delta\rho_2 = B_0 \tau_2^{\beta}, \quad K_2 = \frac{(x(1-x)}{T_C(x)} \frac{dT_C}{dx},$$

$$\tau = \frac{T-T_C}{T}, \quad \Delta\rho = \frac{\rho-\rho_C}{\rho_C}. \tag{1}$$

The key parameter values were obtained from the following sources: the derivative $\frac{dT_C}{dx} = -3.25$ is from the critical temperature curve equation

reported by Marshall and Simonson [3]; the critical temperature for composition $x = 0.5$ mole fraction of D_2O, $T_C = 645.472$ K is also from Ref. 3; the critical amplitudes $A_0^+ = 33.325$ and $B_0 = 1.952$ of the power laws for the isochoric heat capacity and coexistence curve are from Ref. 8; and the universal critical exponents for C_V, $\alpha = 0.112$, and for the coexistence curve, $\beta = 0.325$, are from Ref. 23. At $\tau \ll \tau_2$ the isochoric heat capacity behavior for a binary mixture will be renormalized by a factor $1/(1-\alpha)$, referred to as Fisher renormalization [22]. In terms of density, along the critical isotherm the behavior of the isochoric heat capacity will be renormalized at densities $|\Delta\rho| \ll \Delta\rho_2$. The values of K_2, τ_2, and $\Delta\rho_2$ calculated from Eq. (1) for an equimolar $H_2O + D_2O$ mixture are -1.259×10^{-3}, 1.532×10^{-33}, and 2.164×10^{-11}, respectively. As one can see, the values of τ_2 and are very small. Therefore, Fisher renormalization of the critical exponent for C_V cannot be experimentally observed, and the isochoric heat capacity of the equimolar $H_2O + D_2O$ mixture behaves like that of pure components as shown in Fig. 4. Figure 9 shows measured and calculated values of C_V for the equimolar $H_2O + D_2O$ mixture along the critical isochore as a function of ln τ. As shown by Fig. 9, the calculated and measured values of C_{VX} differ by a small systematic quantity, and the mixture

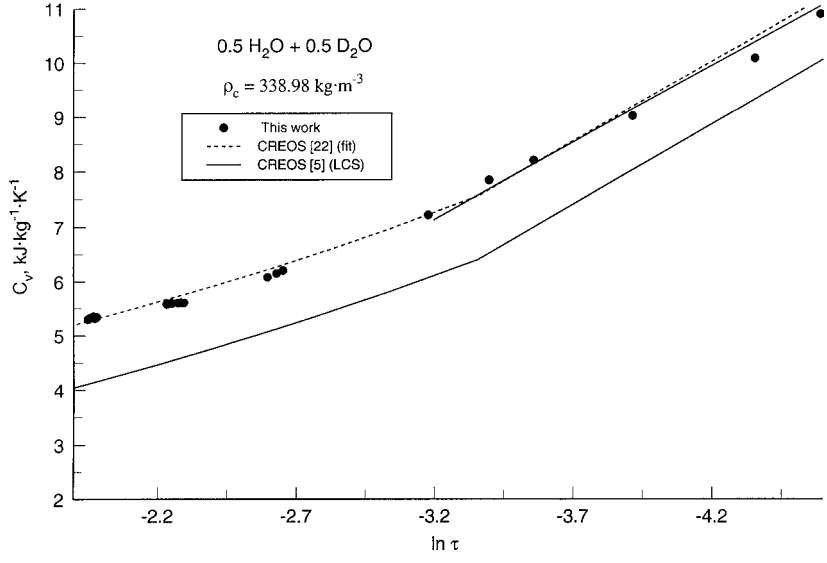

Fig. 9. Isochoric heat capacity of a 0.5 $H_2O + 0.5$ D_2O mixture on the critical isochore 338.98 kg·m^{-3} as a function of ln τ together with values calculated from the CREOS [21] (fitted to experimental data, dashed curve) and the original LCS crossover equation of state by Kiselev et al. [5] (solid curve).

behaves like that of the pure components. Therefore, a correction of the regular part of the LCS crossover model is able to correctly represent the measured values of C_{VX} for the mixture.

4. CONCLUSIONS

Isochoric heat capacity measurements were reported for an equimolar H_2O+D_2O mixture in the temperature range from 391 to 655 K, at seven near-critical densities, namely, 274.05, 299.58, 318.07, 334.78, 338.98, 352.11, and 385.36 $kg \cdot m^{-3}$. A high-temperature, high-pressure adiabatic calorimeter was used. These measurements covered one-phase and two-phase conditions, and were reported on the coexistence curve. The results of the isochoric heat capacity and saturated density measurements were compared with values calculated with crossover models. The critical parameters (the critical temperature and the critical density) derived from the C_V measurements using the quasi-static thermograms technique are in good agreement with the values reported by Marshall and Simonson [3] for the critical temperature. Uncertainties of the C_V measurements are estimated to be within $\pm 2\%$. The liquid and vapor one-phase isochoric heat capacities, temperatures, and saturation densities were extracted from experimental data for each measured isochore. The measured results were used to analyze the critical behavior of the isochoric heat capacity of an equimolar H_2O+D_2O mixture in terms of the principle of isomorphism of critical phenomena. The analysis showed that experimental isochoric heat capacity data exhibit a weak singularity similar to that observed for the pure components. The fact that the Fisher renormalization for the C_V of mixtures of H_2O and D_2O is not experimentally observable has been pointed out by Abdulkadirova et al. [1]. To confirm reliability of the measurement method, the isochoric heat capacity for light water was measured on the critical isochore (321.96 $kg \cdot m^{-3}$) in both the one- and two-phase regions. The result for the phase transition temperature ($T_{C,\,\text{this work}} = 647.104 \pm 0.003$ K) is in good agreement with the value ($T_{C,\,\text{IAPWS}} = 647.096$ K) for the critical temperature adopted by IAPWS. To improve the representation of the new $PVTx$ reported by Bazaev et al. [4] and the present C_VVTx results, only the parameters of the regular background part of the crossover model by Kiselev et al. [5] needed to be refit to the new data.

ACKNOWLEDGMENTS

The authors thank Profs. J. V. Sengers and S. B. Kiselev for providing calculated values of isochoric heat capacity and saturated density data for

the equimolar H_2O+D_2O mixture and for their interest in this work. One of us (I.M.A.) thanks the Physical and Chemical Properties Division of the National Institute of Standards and Technology for the opportunity to work as a Guest Researcher at NIST during the course of this research. This work was supported by RFBR Grant 00-02-17856.

REFERENCES

1. Kh. S. Abdulkadirova, A. Kostrowicka Wyczalkowska, M. A. Anisimov, and J. V. Sengers, *J. Chem. Phys.* **116**:4597 (2002).
2. J. M. Simonson, *J. Chem. Thermodyn.* **22**:739 (1990).
3. W. L. Marshall and J. M. Simonson, *J. Chem. Thermodyn.* **23**:613 (1991).
4. A. R. Bazaev, I. M. Abdulagatov, J. W. Magee, E. A. Bazaev, and A. E. Ramazanova, *J. Supercritical Fluids* (in press).
5. S. B. Kiselev, I. M. Abdulagatov, and A. H. Harvey, *Int. J. Thermophys.* **20**:563 (1999).
6. A. Kostrowicka Wyczalkowska, Kh. S. Abdulkadirova, M. A. Anisimov, and J. V. Sengers, *J. Chem. Phys.* **113**:4985 (2000).
7. N. G. Polikhronidi, I. M. Abdulagatov, J. W. Magee, and G. V. Stepanov, *Int. J. Thermophys.* **22**:189 (2001).
8. N. G. Polikhronidi, I. M. Abdulagatov, J. W. Magee, and G. V. Stepanov, *Int. J. Thermophys.* **23**:745 (2002).
9. S. B. Kiselev and D. G. Friend, *Fluid Phase Equil.* **155**:33 (1998).
10. W. Wagner and A. Pruss, *J. Phys. Chem. Ref. Data* **31**:387 (2002).
11. N. G. Polikhronidi, R. G. Batyrova, and I. M. Abdulagatov, *Fluid Phase Equil.* **175**:153 (2000).
12. N. B. Vargaftik, *Handbook of Physical Properties of Liquids and Gases*, 2nd Ed. (Hemisphere, New York, 1983).
13. N. G. Polikhronidi, I. M. Abdulagatov, and R. G. Batyrova, *Fluid Phase Equil.* (in press).
14. Kh. I Amirkhanov, G. V. Stepanov, and B. G. Alibekov, *Isochoric Heat Capacity of Water and Steam* (Amerind, New Delhi, 1974).
15. A. M. Kerimov, Ph.D. thesis (Azneftechim, Baku, Azerbaijan, 1964).
16. I. M. Abdulagatov, V. I. Dvoryanchikov, and A. N. Kamalov, *J. Chem. Eng. Data* **43**:830 (1998).
17. B. A. Mursalov, I. M. Abdulagatov, V. I. Dvoryanchikov, and S. B. Kiselev, *Int. J. Thermophys.* **20**:1497 (1999).
18. I. M. Abdulagatov, V. I. Dvoryanchikov, and B. A. Mursalov, *Fluid Phase Equilib.* **143**:213 (1998).
19. N. G. Polikhronidi, R. G. Batyrova, I. M. Abdulagatov, and J. W. Magee, to be submitted to *Fluid Phase Equilib.*
20. I. K. Kamilov, G. V. Stepanov, I. M. Abdulagatov, A. R. Rasulov, and E. I. Milikhina, *J. Chem. Eng. Data.* **46**:1556 (2001).
21. S. B. Kiselev, New parameters of the regular part of crossover equation of state derived from fitting the present C_V data were provided by S. B. Kiselev (Chemical Engneering Department, Colorado School of Mines, Golden, Colorado 80401-1887).
22. M. E. Fisher, *Phys. Rev.* **176**:237 (1968).
23. J. V. Sengers and J. M. H. Levelt Sengers, Critical phenomena in classical fluids, in *Progress in Liquid Physics*, C. A. Croxton, ed. (Wiley, New York, 1978), p. 103.